Energy & Buildings 202 (2019) 109376

Contents lists available at ScienceDirect

Energy & Buildings

journal homepage: www.elsevier.com/locate/enbuild

Smart utilization of solar energy with Optic-Variable Wall (OVW) for thermal comfort

Ye Zhu [a], Cheng Wang [b,*], Xiaofeng Guo [c,d,**]

[a] Jiangsu Key Laboratory of Fine Petrochemical Engineering, Changzhou University, Changzhou, 213164, Jiangsu, PR China
[b] Jiangsu Provincial Key Laboratory of Oil & Gas Storage and Transportation Technology, Changzhou University, Changzhou, 213016, Jiangsu, PR China
[c] Université Paris Diderot, Sorbonne Paris Cite, LIED, UMR 8236, CNRS, F-75013, Paris, France
[d] ESIEE Paris, Université Paris Est, 2 boulevard Blaise Pascal - Cite Descartes, F-93162, Noisy Le Grand, France

ARTICLE INFO

Article history:
Received 4 March 2019
Revised 5 July 2019
Accepted 14 August 2019
Available online 15 August 2019

Keywords:
Optic-Variable Wall (OVW)
Optic-Fixed Wall (OFW)
Solar energy
Thermal comfort

ABSTRACT

Smart utilization of solar energy with OVW (Optic-Variable Wall) for thermal comfort is verified. The application of OVW in passive buildings is discussed. With no active heating & cooling measure adopted for building located in Shanghai, OVW can offer relatively comfortable environment in the whole year period. Compared with reflective OFW (Optic-Fixed Wall with high reflectivity), the cold period in winter is shortened and meanwhile the summer is kept cool. Compared with absorptive OFW (Optic-Fixed Wall with low reflectivity), the hot period in summer is enormously suppressed and the winter is kept warm. The performance of thermal comfort, e.g. Discomfort Hours, Discomfort-Degree Hours and Discomfort Degree, is significantly improved. Comparing with OFW, both reflective and absorptive, less discomfort hours and less discomfort-degree hours are concluded with the adoption of OVW. The average discomfort-degree of OVW is the least in summer as well as in winter, although the average discomfort-degree in the whole-year period is slightly larger than absorptive OFW. It is also concluded that absorptive OFW performs better than reflective OFW on Discomfort-Degree Hours, but worse on Discomfort Hours. The results are also meaningful for other applications, such as vehicles and light-steel-structured industrial warehouse.

1. Introduction

With the development of society, the issues of energy-consumption as well as environment pollution have attracted more and more attentions [1,2]. Buildings account for almost one third of the total energy consumption in the world, mainly consumed in HVAC system for indoor air control [3–5]. Therefore, passive measures, such as heavy thermal mass or strong thermal insulation [6–12], effective ventilation strengthened with solar power [13–17], utilization or management of solar radiation [18–20], etc., are widely adopted in green (low-carbon) building design.

Among these methods, utilization or management of solar radiation is of the most interest to designers, engineers as well as scientists [21–26], since it has the least influence on the structure of buildings. Moreover, to some extent, it can help release some restrictions on the design of buildings, for the sake of energy-saving. For instance, more freedom is available to adopt glass curtain or window to offer brighter indoor atmosphere or better sight-viewing [27–30], instead of the constraint of the window-to-wall ratio (WWR) [31,32].

The utilization of solar radiation includes the technologies of PV/PT/PVT [33–37] and trombe-wall [38–40] as well as the enhancement on ventilation [14,15,17]. Among these technologies, PV is to some extent most attractive, due to its compatibility with electric-devices in HVAC. Moreover, it meets the trend of smart grid infrastructure-construction. Luthander et al. [41] reviewed on the self-consumption of PV electricity in buildings. It is proposed that the behavioral responses and the impact on the distribution grid still need to be studied. Moreover, comparing with PT technology, PV system calls for large capital investment of electricity-storage units and suffers from the short-term life of batteries as well as the performance degradation issues. As a matter of fact, most of these technologies cannot well fit the demand of HVAC load in the whole year period, due to the energy gap between heating/cooling power in demand and solar power in supply. That is to say, in summer, when the solar radiation is strong, the energy in demand is in the form of cooling power; however, in winter, the heating power is favored, while the solar radiation is weak. Moreover, the solar radiation is one important source of cooling load in

* Corresponding author.
** Corresponding author.
E-mail addresses: wangcheng3756@163.com (C. Wang), xiaofeng.guo@esiee.fr (X. Guo).

https://doi.org/10.1016/j.enbuild.2019.109376
0378-7788/

Nomenclature

ADD	Average Discomfort Degree-Hours, d·°C·y^{-1}
ADDc	Average Over-Cooling Discomfort Degree-Hours, d·°C·y^{-1}
ADDh	Average Over-Heating Discomfort Degree-Hours, d·°C·y^{-1}
C	Thermal capacity, J·kg^{-1}·K^{-1}
DDH	Discomfort Degree-Hours, d·°C·y^{-1}
DDHc	Over-Cooling Discomfort Degree-Hours, d·°C·y^{-1}
DDHh	Over-Heating Discomfort Degree-Hours, d·°C·y^{-1}
DH	Discomfort Hours, h
DHc	Over-Cooling Discomfort Hours, h
DHh	Over-Heating Discomfort Hours, h
h	Heat transfer coefficient, W·m^{-2}·K^{-1}
I	Solar radiation, W·m^{-2}
MDDc	Maximum Over-Cooling Discomfort Degree, °C
MDDh	Maximum Over-Heating Discomfort Degree, °C
t	Time, s
T	Temperature, °C
x	Position, m

Subscript

1	Parameter at onset temperature
2	Parameter at offset temperature
80	80% of satisfactory
90	90% of satisfactory
ai	Indoor air
ao	Outdoor air
H	Horizontal surface
H80	Upper limit for 80% of satisfactory
H90	Upper limit for 90% of satisfactory
i	Inside
L80	Lower limit for 80% of satisfactory
L90	Lower limit for 90% of satisfactory
o	Outside
s1	Onset for optic-variation
s2	Offset for optic-variation
V	Vertical surface
wl	Wall layer

Greek symbol

β	Reflectivity
δ	Thickness, m
λ	Thermal conductivity, W·m^{-1}·K^{-1}
ρ	Density, kg·m^{-3}

buildings. Therefore, it is necessary to manage the transformation of solar radiation into heat source, e.g. less in summer and more in winter.

Shadowing is one normal way to conduct the management of solar radiation [42,43]. When solar radiation is strong in summer, it is possible to keep the indoor atmosphere cool by utilization of solar shadowing to block the inlet of solar radiation. However, it is invalid for heating in winter. Recently, radiation cooling technology is developed [44–48]. Goldstein et al. [46] reported that with the radiative sky cooling, heat is passively rejected into space through transparent windows, and results in the sub-ambient cooling. Mandal et al. [49] reported a simple, inexpensive and scalable phase inversion-based method for fabricating hierarchically porous P(VdF-HFP)HP coating. The reflectance is reported as 0.96 ± 0.03 and the long-wave infrared emittance is reported as 0.97 ± 0.02. The sub-ambient cooling power is approximately 100 W·m^{-2}. The principle is that when the radiation wavelength is kept at certain range with delicate structure design, the sky or aerospace could be applied as the cooling source, therefore, the buildings are kept cool in summer. Unfortunately, the enhancement of heating in winter is not reported. Similarly, the cool roof or green roof technologies are also only valid for the hot weather, even in some cases, at the cost of heating load penalty. Uemoto et al. [50] estimated the thermal performance of cool colored paints, containing reflective pigments. The experimental results indicate that more than 10 °C of surface temperature repression is obtained, comparing with conventional paintings. As a result, the benefits of thermal comfort improvement as well as air conditioning costs reduction are predicted. Castleton et al. [51] reviewed the application of green roofs in building energy saving and the potential for retrofit in UK. However, the issue of heavy-duty maintenance as well as the damage to the building structure should be paid more attention to. Besides, the dual-colored curtain is reported to keep air temperature inside the building, located in the North of China, cool in summer and warm in winter [52,53]. However, it is under the control of mechanic adjustment, therefore, it is not possible to follow the variation of atmosphere in time. Correspondingly, heavy thermal mass is, to the most extent, necessary to keep promise the performance of passive buildings. However, heavy thermal mass is not favored in some cases, from the viewpoint of other technical fields, such as the issue of self-weight or structure-strengthen.

OVW (Optic-Variable Wall), also naming as thermochromic coating or painting, is the technology to automatically adjust the reflection/absorption of solar radiation on surface (e.g. wall or roof in buildings), as shown in Fig. 1, responding to the variation of surface status, such as temperature. Since the surface temperature is corresponding to the ambient temperature and the solar radiation, it is possible to reflect the effects of bi-parameters on the HVAC load in buildings. As far as the thermochromic principle and performance enhancement, Hajzeri et al. [54] investigated the influence of developer on structural, optical and thermal properties of a benzofluoran-based thermochromic composite. Karlessi and Santamouris [55] investigated the performance of thermochromic coatings with exposure to UV and tested the aging property with filters. It is believed that most of the protection is due to the cut-off of spectrum with wavelength shorter than 600 nm. Since there is no mechanism control, OVW can theoretically trace the rapid variation of meteorological information, i.e. ambient temperature as well as solar radiation. It is reported that OVW has the potential to simultaneously keep the indoor air cool in summer and warm in winter [56,57]. However, to the most of our knowledge, the performance of OVW in the whole year period on thermal comfort control are not comprehensively reported, especially when only the passive measures are applied.

In this paper, the application of OVW in passive buildings is discussed. The profile of annual indoor air temperature and the evaluation of thermal comfort are discussed in details. The results offer new sight-viewing on the application of OVW and another choice for energy-saving and thermal-comfort control as well as green (low-carbon) design in vehicles and light-steel-structured industrial warehouse.

2. Physical model

2.1. Heat transfer process

The typical model, i.e. a light-weight warehouse, as well as the heat transfer process is shown in Fig. 2. Vertical wall or horizontal roof is taken as the object for indoor air temperature assessment in the building, located in Shanghai, which has a typical subtropical humid climate in the East of China. The meteorological data is cited from ASHARE and transient heat transfer model is applied. No active measures is conducted, aiming at the goal of

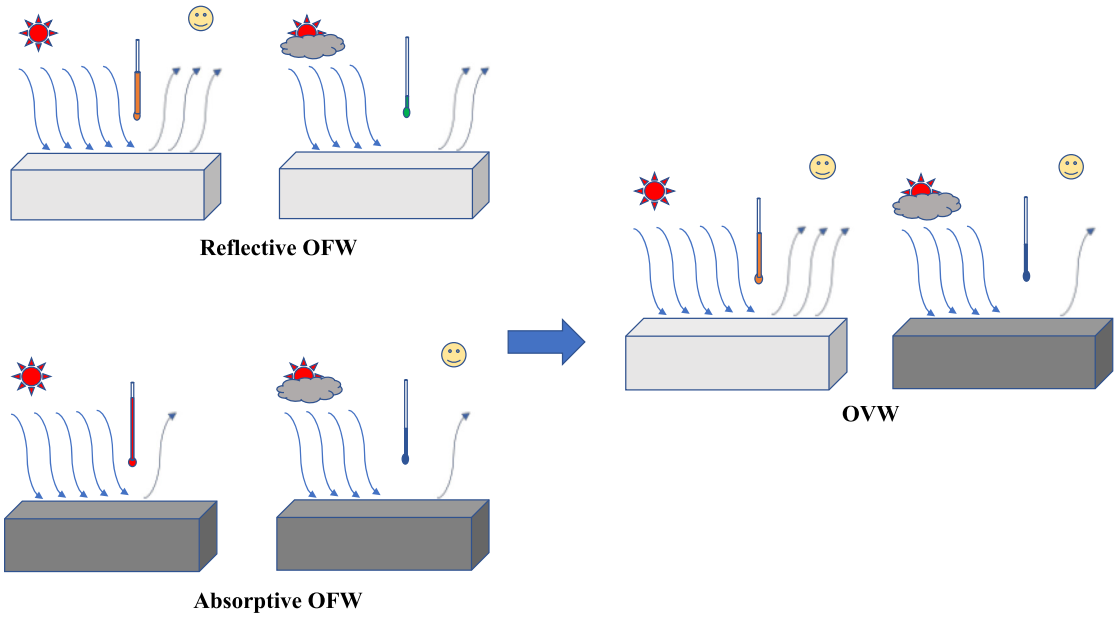

Fig. 1. Principle of Optic-Variable Wall (OVW).

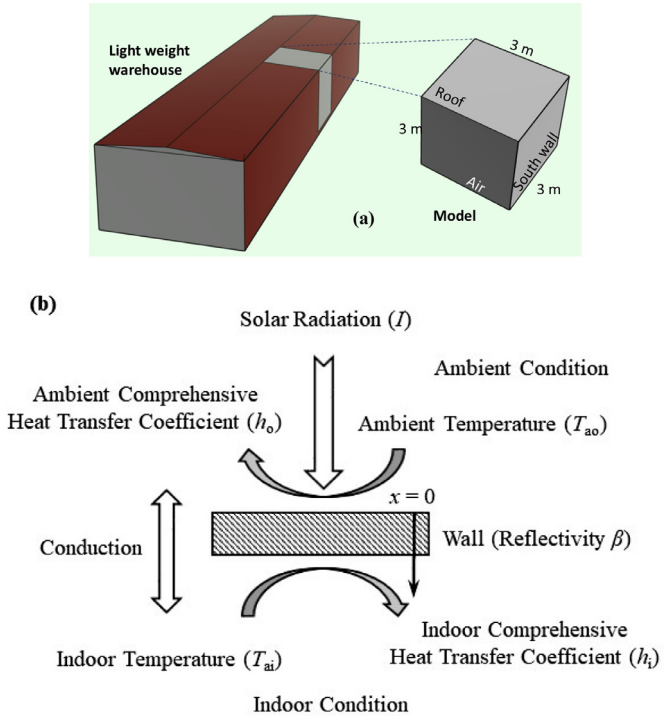

Fig. 2. Physical Model of OVW, (a) Warehouse and the studied model and (b) Heat flux for a horizontal roof / vertical wall.

zero-energy-consumption. To make clear the effects of OVW, insulation layer is neglected in analysis.

The light weight warehouse is symmetrized along the east-west line, the length of which is around 20 m. The warehouse is approximately 6 m wide in the north and south orientation. In this manuscript, the south wall and the roof are concerned as the object in analysis. Due to the symmetry structure as well as the relative large size in east-west line, a cubic physical model with side length of 3 m, as shown in the right part of Fig. 2a, is peeled out and evaluated with the thermal comfort.

Due to the principle of OVW, the reflection of solar radiation on OVW corresponds to the outside surface temperature of wall-layer. At low temperature, OVW shows weak reflection to solar radiation, while it offers strong reflection at high temperature [56]. For comparison, the results of indoor air temperature (*IAT*) with two kinds of OFW (Optic-Fixed Wall), i.e. with the corresponding high and low reflectivity, are also assessed.

Lumped indoor air temperature T_{ai} is determined by:

$$(\rho_{ai} \cdot C_{ai} \cdot \delta_{ai}) \cdot \frac{dT_{ai}}{dt} = h_i \cdot \left(T_{wl}|_{x=\delta_{wl}} - T_{ai}\right) \tag{1}$$

where ρ_{ai}, C_{ai} and δ_{ai} refer to the density, heat capacity and equivalent size of indoor air, respectively. h_i is corresponding to the indoor comprehensive heat transfer coefficient, taking into consideration of convection as well as radiation heat transfer.

Wall layer temperature T_{wl} is expressed as:

$$(\rho_{wl} \cdot C_{wl}) \cdot \frac{\partial T_{wl}}{\partial t}|_{x\in(0,\delta_{wl})} = \lambda_{wl} \cdot \frac{\partial^2 T_{wl}}{\partial x^2}|_{x\in(0,\delta_{wl})} \tag{2a}$$

and

$$-\lambda_{wl} \cdot \frac{\partial T_{wl}}{\partial x}|_{x=0} = h_o \cdot (T_{ao} - T_{wl}|_{x=0}) + (1-\beta) \cdot I \tag{2b}$$

$$-\lambda_{wl} \cdot \frac{\partial T_{wl}}{\partial x}|_{x=\delta_{wl}} = h_i \cdot \left(T_{wl}|_{x=\delta_{wl}} - T_{ai}\right) \tag{2c}$$

where ρ_{wl} is the density of wall-layer. C_{wl} corresponds to the heat capacity of wall-layer. λ_{wl} refers to the thermal conductivity of wall-layer. h_o is the comprehensive heat transfer coefficient between wall-layer and ambient, with the consideration of convection as well as radiation heat transfer.

The reflectivity β is determined by outside surface temperature of wall-layer $T_{wl}|_{x=0}$:

$$\beta = \begin{cases} \beta_1 & T_{wl}|_{x=0} \le T_{s1} \\ \beta_1 + \frac{T_{wl}|_{x=0} - T_{s1}}{T_{s2} - T_{s1}} \cdot (\beta_2 - \beta_1) & T_{s1} \le T_{wl}|_{x=0} \le T_{s2} \\ \beta_2 & T_{wl}|_{x=0} \ge T_{s1} \end{cases} \tag{3}$$

where T_{s1} and T_{s2} refer to the onset and offset temperature of optic-variation, respectively. β_1 and β_2 corresponds to the reflectivity of OVW at T_{s1} and T_{s2}, respectively. β_1 is smaller than β_2, and the ideal value is ranging from 0.1 to 0.9, implying that

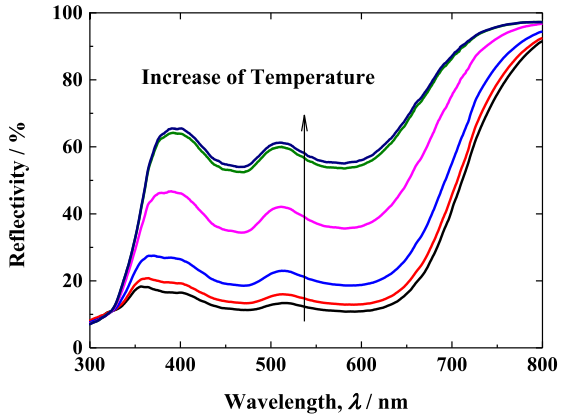

Fig. 3. Solar reflectivity with increasing surface temperature in structure with OVW.

Table 1
Relevant parameters in the theoretical model.

ρ_{ai}	1 kg·m^{-3}
ρ_{wl}	7800 kg·m^{-3}
C_{ai}	1000 J·kg^{-1}·K^{-1}
C_{wl}	500 J·kg^{-1}·K^{-1}
δ_{ai}	3 m
δ_{wl}	3 mm
λ_{wl}	4 W·m^{-1}·K^{-1}
h_i	10 W·m^{-2}·K^{-1}
h_o	30 W·m^{-2}·K^{-1}
T_{s1}	23.5 °C [57]
T_{s2}	26.5 °C [57]

Note: T_{s1} and T_{s2} are designated according to the optimal results in ref. [56,58].

$\beta_1 = 0.1$ and $\beta_2 = 0.9$. The results of reflectivity in structure with OVW at increasing surface temperature, measured with UV-3600 (Shimadzu) are depicted in Fig. 3, verifying the increment of solar reflectivity with temperature. As for the practical coating, it is estimated that the reflectivity varies from 0.1 to around 0.6, which might be further increased by doping or mixing, etc.

The initial state is assumed thermal-equilibrium and expressed as:

$$T_{ao}|_{t=0} = T_{wl}|_{t=0} = T_{ai}|_{t=0} \tag{4}$$

The relevant parameters in the model are summarized in Table 1.

2.2. Thermal comfort assessment

Due to the merit of building with passive measures, the thermal comfort degree is assessed with the deviation of indoor temperature from the set temperature, which is linked with the ambient temperature, as shown in Eq. (5). The deviation criterion has two indices, i.e. the time span (Discomfort Hour), expressed in Eq. (6) and the product of time span and temperature deviation (Discomfort Degree-Hour), expressed in Eq. (7).

2.2.1. Acceptable indoor air temperature

According to the ASHARE adaptive comfort model [59], the thermal comfortable indoor air temperature is expressed as:

$$T_{ai} = 18.9 + 0.255 \cdot T_{ao} \tag{5a}$$

The temperature zone of indoor air for 90% of satisfactory is determined by:

$$T_{L90} \le T_{ai} \le T_{H90} \tag{5b}$$

where T_{L90} and T_{H90} refer to the lower and upper limit of T_{ai} for 90% of satisfactory.

$$T_{L90} = 16.11 + 0.255 \cdot T_{ao} \tag{5c}$$

and

$$T_{H90} = 21.69 + 0.255 \cdot T_{ao} \tag{5d}$$

The temperature zone of indoor air for 80% of satisfactory is determined by:

$$T_{L80} \le T_{ai} \le T_{H80} \tag{5e}$$

where T_{L80} and T_{H80} refer to the lower and upper limit of T_{ai} for 80% of satisfactory.

$$T_{L80} = 15.63 + 0.255 \cdot T_{ao} \tag{5f}$$

and

$$T_{H80} = 22.17 + 0.255 \cdot T_{ao} \tag{5g}$$

2.2.2. Discomfort Hours

Summarizing the time span when the indoor air temperature lies out of the thermal comfort range, as described in Eq. (5), the Discomfort Hours *DH* as well as the over-heated *DHh* and over-cooled *DHc* are determined for 80% and 90% of satisfactory, as shown in Eq. (6).

$$DH_{90} = DHh_{90} + DHc_{90} \tag{6a}$$

and

$$DH_{80} = DHh_{80} + DHc_{80} \tag{6b}$$

$$DHh_{90} = \sum_{T_{ai} \ge T_{H90}} dt \tag{6c}$$

and

$$DHh_{80} = \sum_{T_{ai} \ge T_{H80}} dt \tag{6d}$$

$$DHc_{90} = \sum_{T_{ai} \le T_{L90}} dt \tag{6e}$$

and

$$DHc_{80} = \sum_{T_{ai} \le T_{L80}} dt \tag{6f}$$

2.2.3. Discomfort Degree-Hours

Summarizing the product of indoor air temperature deviation and the corresponding time span leads to the Discomfort Degree-Hours *DDH* as well as *DDHh* and *DDHc* for 80% and 90% of satisfactory, as shown in Eq. (7).

$$DDH_{90} = DDHh_{90} + DDHc_{90} \tag{7a}$$

and

$$DDH_{80} = DDHh_{80} + DDHc_{80} \tag{7b}$$

$$DDHh_{90} = \sum_{T_{ai} \ge T_{H90}} (T_{ai} - T_{H90}) \cdot dt \tag{7c}$$

and

$$DDHh_{80} = \sum_{T_{ai} \ge T_{H80}} (T_{ai} - T_{H80}) \cdot dt \tag{7d}$$

$$DDHc_{90} = \sum_{T_{ai} \le T_{L90}} (T_{L90} - T_{ai}) \cdot dt \tag{7e}$$

and

$$DDHc_{80} = \sum_{T_{ai} \le T_{L80}} (T_{L80} - T_{ai}) \cdot dt \tag{7f}$$

2.2.4. Maximum and average Discomfort Degree

The maximum Discomfort Degree, i.e. *MDDh* and *MDDc* are expressed as:

$$MDDh_{90} = \max\left(T_{ai} - T_{H90}\right) \tag{8a}$$

and

$$MDDh_{80} = \max\left(T_{ai} - T_{H80}\right) \tag{8b}$$

$$MDDc_{90} = \max\left(T_{L90} - T_{ai}\right) \tag{8c}$$

and

$$MDDc_{80} = \max\left(T_{L80} - T_{ai}\right) \tag{8d}$$

The average Discomfort Degree, i.e. *ADDh* and *ADDc* are expressed as:

$$ADD_{90} = \frac{DDH_{90}}{DH_{90}} \tag{9a}$$

and

$$ADD_{80} = \frac{DDH_{80}}{DH_{80}} \tag{9b}$$

$$ADDh_{90} = \frac{DDHh_{90}}{DHh_{90}} \tag{9c}$$

and

$$ADDh_{80} = \frac{DDHh_{80}}{DHh_{80}} \tag{9d}$$

$$ADDc_{90} = \frac{DDHc_{90}}{DHc_{90}} \tag{9e}$$

and

$$ADDc_{80} = \frac{DDHc_{80}}{DHc_{80}} \tag{9f}$$

3. Results and discussion

Single passive measure is conducted with OVW. The comparison corresponds to OVW and OFW with low or high reflectivity. The performance indicator is the thermal comfort degree, determined by Eqs. (6)–(9).

The time span is taken as the continuous years. The ambient temperature as well as the solar radiation on horizontal and vertical surface are depicted in Fig. 4. The warehouse is located in Shanghai. The highest and lowest ambient temperature is 35.3 °C in summer and −6.4 °C in winter, respectively. The strongest solar radiation on horizontal and vertical surface is around 1000 W·m^{-2} in summer and 900 W·m^{-2} in winter, respectively.

The comparison is independently conducted for both the horizontal roof and the vertical walls. The onset and offset temperatures for optic-variation, i.e. T_{s1} and T_{s2} are prescribed as 23.5 °C and 26.5 °C, respectively. The low and high reflectivity of OFW is prescribed as 0.1 and 0.9, respectively. Correspondingly, the reflectivity of OVW varies from 0.1 at temperature lower than T_{s1} to 0.9 at temperature higher than T_{s2}.

3.1. Indoor air temperature (IAT)

The variation of indoor air temperature T_{ai} in continuous years is depicted in Fig. 5 and Table 2. It is concluded that the range of T_{ai} is narrower in the case of OVW, rather than both cases of OFW. The peak temperature of OVW in summer is close to that of OFW with high reflectivity (reflective OFW), while the valley temperature of OVW in winter is close to that of OFW with small reflectivity (absorptive OFW). Therefore, it is favored to adopt OVW

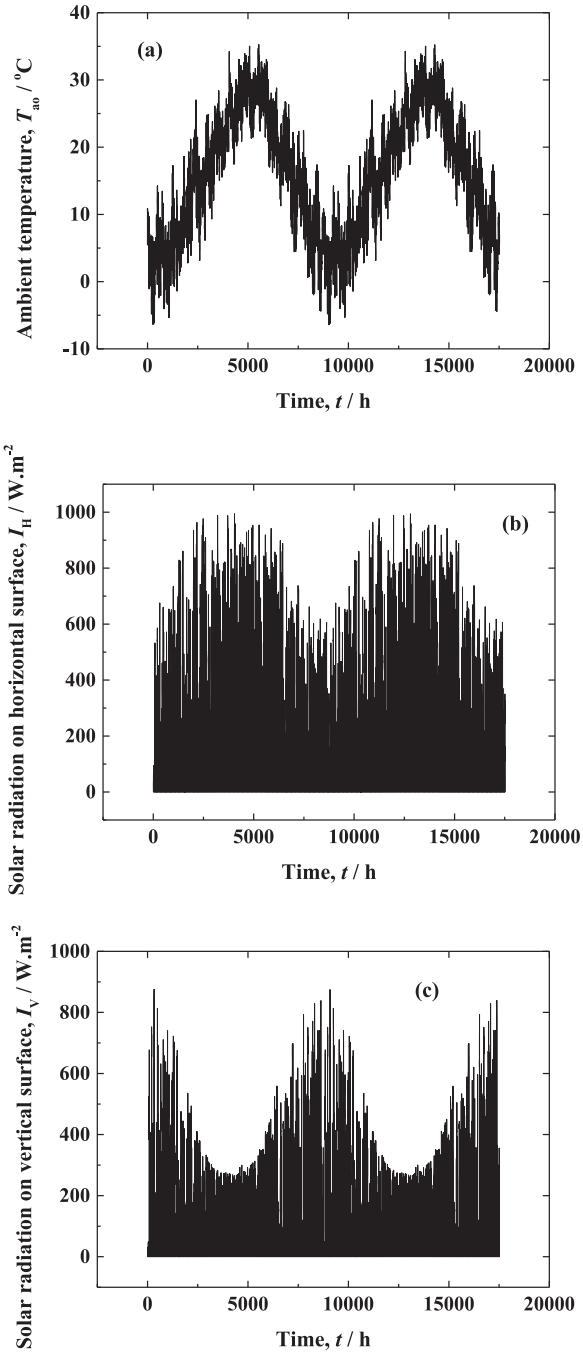

Fig. 4. Profile of ambient temperature and solar radiation on horizontal and vertical surfaces. (a) Ambient temperature T_{ao}; (b) Horizontal solar radiation I_H and (c) Vertical solar radiation I_V.

Table 2
Comparison of maximum and minimum *IAT*.

	Maximum *IAT* / °C		Minimum *IAT* / °C	
	Horizontal	Vertical	Horizontal	Vertical
OVW	*28.69*	*28.30*	***4.60***	***4.60***
Reflective OFW	**28.60**	**28.22**	3.59	3.58
Absorptive OFW	33.81	30.39	**4.60**	**4.60**

Note: Red-Bond-Mark value corresponds to the best performance of IAT. Inclined-Mark value corresponds to the results of OVW.

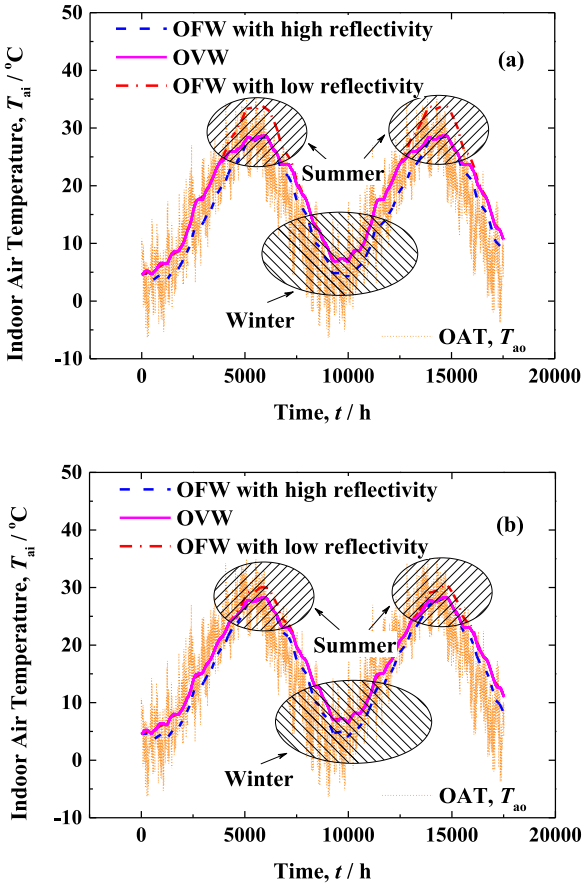

Fig. 5. Variation of indoor air temperature T_{ai}, (a) Horizontal surface and (b) Vertical surface.

to keep the air temperature inside stable and comfortable in the whole year. Instead, the adoption of OFW may be over-heated, in the case of absorptive OFW, or over-cooled, in the case of reflective OFW.

During the period between summer and winter, the variation of IAT in the case of OVW is more similar to absorptive OFW. In the whole year, OVW offers more comfortable indoor condition, which is neither too hot nor too cold.

Comparing Fig. 5a with b, it is also found that, due to the relatively strong solar radiation, the difference of T_{ai} among OFW, i.e. absorptive and reflective, and OVW walls is more obvious on horizontal surface, such as the roof. The effects of OVW on IAT control is, therefore, more significant on horizontal surface.

It is concluded from Table 2 that the maximum *IAT* of OVW is close to that of reflective OFW, which offers the best result among the three models. Comparing with absorptive OFW, the maximum *IAT* is reduced approximately by approximately 5 °C and 2 °C on horizontal and vertical surfaces, respectively. On the other hand, the minimum *IAT* of OVW is the same as that of absorptive OFW, which offers the best results among the three models, and is increased by 1 °C, comparing with reflective OFW. The results of *IAT* with OVW are almost within the range of 5–30 °C, which is acceptable for NR (Non-Residential) buildings without HVAC systems.

3.2. Discomfort Hour

The results of Discomfort Hour are depicted in Figs. 6 and 7. Besides, two index of discomfort hour is proposed for positive and negative deviation, as shown in Eqs. (7c)–(7d) and (7e)–(7f), respectively.

It is obvious that, OVW offers the best performance of thermal-comfort, while absorptive OFW shows the worst results. For instance, on the horizontal surface, CH_{90} of OVW is 41.76% of the whole year, which is 1.37 and 2.09 times of reflective and absorptive OFW, respectively. However, on the vertical surface, due to the relative weak solar radiation, the effects of OVW are not so much obvious. CH_{90} of OVW is only 1.17 and 1.52 times of reflective and absorptive OFW, respectively. Similar trends are concluded, as far as CH_{80} is concerned.

When the composition of *DH* is taken into consideration, i.e. *DHh* and *DHc*, it is concluded that most of the discomfort hour is over-cooled, which implies not enough heat flux to lift-up the inside air temperature. Since the absorptive OFW offers the best performance of *DHc* and OVW offers similar results, it is concluded that OVW makes the most efforts to help reduce the over-cooled discomfort hour, even though the indoor air is still not comfort.

In the case of *DHh*, the reflective OFW always gives the best results, and OVW shows similar results. For instance, in the case

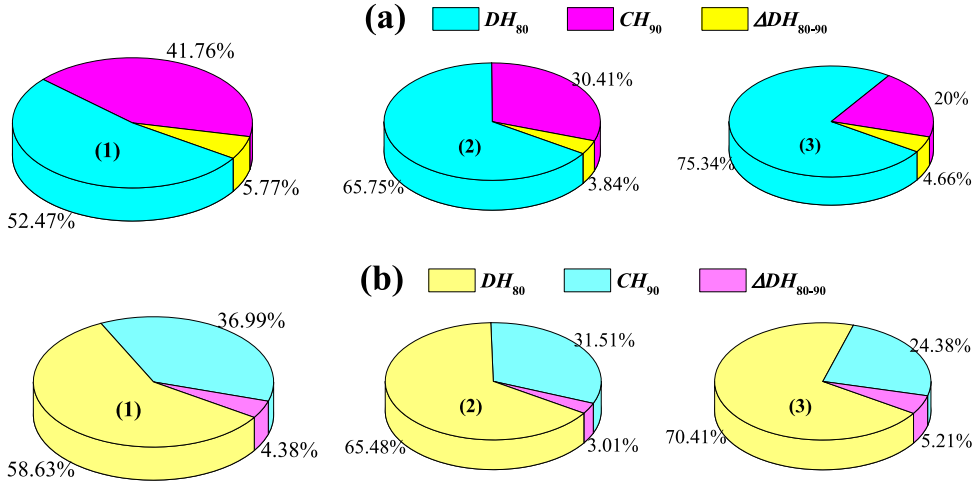

Fig. 6. Comparison of the Discomfort Hour *DH*, (a) Horizontal surface and (b) Vertical surface, (1) OVW, (2) Reflective OFW and (3) Absorptive OFW.
Note: DH_{80} refers to the Discomfort Hour for 80% of satisfactory. CH_{90} refers to the Comfort Hour for 90% of satisfactory, corresponding to the strictest criteria of thermal-comfort. $\Delta DH_{80\text{-}90}$ refers to the increment of Discomfort Hour, when the satisfactory degree is increased from 80% to 90%. The sum of DH_{80} and $\Delta DH_{80\text{-}90}$ corresponds to DH_{90}. The sum of DH_{80}, CH_{90} and $\Delta DH_{80\text{-}90}$ corresponds to the whole year period, i.e. 365days.

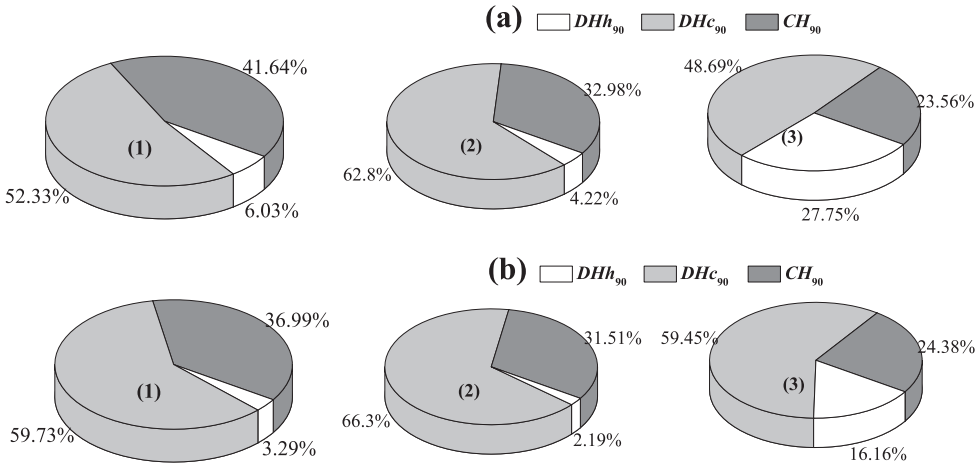

Fig. 7. Comparison of *DHh* and *DHc* for 90% satisfactory, (a) Horizontal surface and (b) Vertical surface, (1) OVW, (2) Reflective OFW and (3) Absorptive OFW.
Note: DHh_{90} and DHc_{90} refer to the over-heated and over-cooled Discomfort Hour for 90% satisfactory, respectively. The sum of DHh_{90} and DHc_{90} corresponds to DH_{90}. The sum of DHh_{90}, DHc_{90} and CH_{90} corresponds to the whole year period, i.e. 365days.

of vertical surface, DHh_{90} with reflective OFW is 8 d·y^{-1}, and the value of DHh_{90} is 12 and 59 d·y^{-1} with OVW and absorptive OFW, respectively. Therefore, OVW also makes the most efforts to help reduce the over-heated discomfort hour, and the results are satisfactory, comparing with those of *DHc*.

3.3. Discomfort Degree-Hours

Beside the Discomfort Hour, Discomfort Degree-Hour is an important index for thermal-comfort, which takes the deviation degree of IAT from the comfort value into account. The comparison of Discomfort-Degree hour is depicted in Fig. 8.

Similar to the results of Discomfort Hour, OVW offers the best Discomfort Degree-Hour. The effects of OVW are more significant on horizontal surface. When OVW is adopted, DDH_{90} on horizontal surface is reduced by 35.0% and 22.6%, and DDH_{90} on vertical surface is reduced by 26.1% and 4.6%, comparing with reflective and absorptive OFW, respectively.

When *DDHh* and *DDHc* are concerned independently, *DDHh* is almost ignorable in the case of OVW and reflective OFW, and not so strong in the case of absorptive OFW. Taken into consideration of *DDHc*, it is found that OVW and absorptive OFW offer similar results.

It is interesting to find that, different from the results of *DH*, absorptive OFW offers better results than reflective OFW. This is mainly due to the fact, most of *DH* is in the form of *DHc*. Absorptive OFW can supply more solar radiation absorption, therefore, the deviation of IAT from thermal-comfort is less in the case of absorptive OFW than reflective OFW.

3.4. Maximum and average Discomfort Degree

The maximum and average discomfort-degree are depicted in Fig. 9 and Table 3. It is concluded that DDh_{max} is smaller than DDc_{max}, implying that over-cooling is much worse than over-heating, in all three models. DDh_{max} is less than 5 °C, while DDc_{max} is around 15 °C.

It is also concluded from Fig. 9a, that on horizontal and vertical surfaces, OVW performs the best on Maximum Discomfort-Degree, both DDh_{max} and DDc_{max}, while OFW can only perform well on either DDh_{max} or DDc_{max}. The difference between OVW and OFW is more obvious on horizontal surface. Considering the effects of surface orientation, it is concluded that absorptive OFW is more sensitive, especially when DDh_{max} is concerned. While in the case of

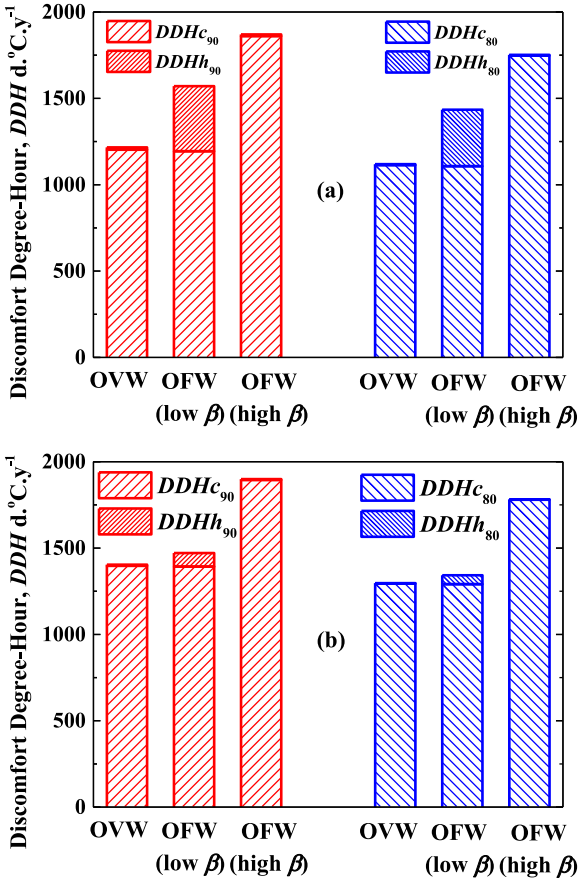

Fig. 8. Comparison of the Discomfort Degree-Hour *DDH*, (a) Horizontal surface and (b) Vertical surface.

DDc_{max}, all three models, i.e. OVW, reflective and absorptive OFW, are little sensitive to the surface orientation.

As far as the average discomfort-degree is concerned, OVW offers the smallest *ADDh* and *ADDc*, among the three models under discussion, as shown in Table 3. However, it is out of expectation that absorptive OFW shows the best *ADD* and reflective OFW offers the worst *ADD*. This is due to the fact that although the reflective OFW reflects the most solar radiation in summer, the

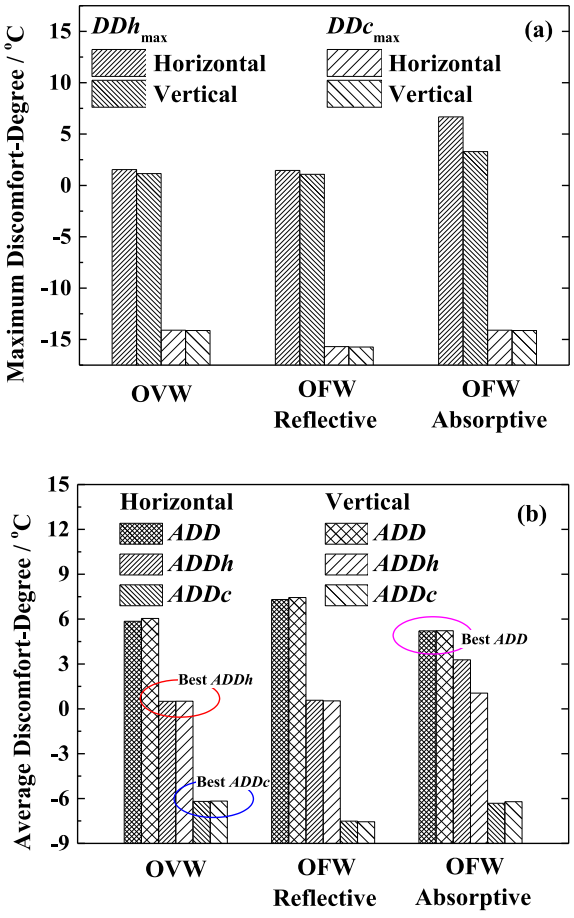

Fig. 9. Comparison of maximum and average discomfort-degree, (a) Maximum Discomfort-Degree and (b) Average Discomfort-Degree.
Note: 80% of satisfactory is considered.

Table 3
Comparison of average discomfort-degree.

	Average Discomfort-Degree / °C					
	Horizontal			Vertical		
	ADD	*ADDh*	*ADDc*	*ADD*	*ADDh*	*ADDc*
OVW	*5.85*	***0.51***	***6.19***	*6.05*	***0.51***	***6.17***
Reflective OFW	7.31	0.57	7.51	7.44	0.53	7.56
Absorptive OFW	**5.21**	3.28	6.32	**5.22**	1.05	6.21

Note: 80% of satisfactory is considered. Red-Bond-Mark value corresponds to the best performance. Inclined-Mark value corresponds to the results of OVW.

major discomfort-hour *DH* is in the form of over-cooling in winter, as shown in Fig. 7 and the maximum over-cooling discomfort-degree DDc_{max} is much larger than DDh_{max}, as shown in Fig. 9.

4. Conclusion

In this paper, the smart utilization of solar radiation with OVW for thermal comfort control is verified. The performance of OVW is assessed and compared with reflective and absorptive OFW, including Indoor Air Temperature (*IAT*), Discomfort Hours (*DH*), Discomfort-Degree Hours (*DDH*) and Discomfort Degree (*DD*). The results offer new sight-viewing on the application of OVW and another choice for energy-saving and thermal-comfort control in buildings as well as green (low-carbon) building design. It is preliminarily verified to design NR (Non-Residential) buildings with OVW, without strong insulation and heavy thermal mass. The following conclusions are made:

(1) With the adoption of OVW, the maximum *IAT* in summer is close to that of reflective OFW, while the minimum *IAT* in winter is close to that of absorptive OFW. On the contrary, the maximum *IAT* of absorptive OFW is 2–5 °C higher, and the minimum *IAT* of reflective OFW is 1 °C lower, comparing with those of OVW.
(2) Discomfort Hours is mainly in the form of over-cooling in Shanghai. With the adoption of OVW, comfort-hour is significantly increased. CH_{90} is increased by approximately 40–100% on horizontal surface and 20–50% on vertical surface, comparing with those of OFW.
(3) The major Discomfort-Degree Hours and the maximum Discomfort Degree are *DDHc* and DDc_{max}, respectively. When the average Discomfort Degree is concerned, the absorptive OFW offers the smallest *ADD*, while the reflective OFW the largest.
(4) When over-heating and over-cooling are considered independently, OVW offers the best performance of average discomfort-degree *ADDh* and *ADDc*, as well as the maximum discomfort-degree DDh_{max} and DDc_{max}.

Therefore, OVW can keep *IAT* low in summer and high in winter, due to its property of tunable reflection on solar radiation. The comfort hour is significantly increased. The average and maximum over-heating and over-cooling discomfort-degree are the best among these three models. The results are also meaningful for other applications, such as vehicles and light-steel-structured spaces. The future works will cover the influences of OVW properties, as well as the integration of OVW with other passive measures.

Declaration of competing interest

The authors declare no conflict of interest in this work.

Acknowledgments

The present work is supported by the National Natural Science Foundation of China (No. 51306023) and the French Ministry of Europe and Foreign Affairs (MEAE), through the PHC Xu Guangqi program (No: 41269UL, 2018) and the Jeunes Talents France Chine program (No: 925116B, 2018). The authors would also like to acknowledge the support from Advanced Catalysis and Green Manufacturing Collaborative Innovation Center of Jiangsu.

References

[1] A.G. Gaglia, C.A. Balaras, S. Mirasgedis, E. Georgopoulou, Y. Sarafidis, D.P. Lalas, Empirical assessment of the Hellenic non-residential building stock, energy consumption, emissions and potential energy savings, Energy Convers. Manag. (2007), doi:10.1016/j.enconman.2006.10.008.
[2] S.A. Kalogirou, Environmental benefits of domestic solar energy systems, Energy Convers. Manag. (2004), doi:10.1016/j.enconman.2003.12.019.
[3] L. Pérez-Lombard, J. Ortiz, C. Pout, A review on buildings energy consumption information, Energy Build. (2008), doi:10.1016/j.enbuild.2007.03.007.
[4] H.X. Zhao, F. Magoulès, A review on the prediction of building energy consumption, Renew. Sustain. Energy Rev. (2012), doi:10.1016/j.rser.2012.02.049.
[5] B. Chenari, J. Dias Carrilho, M. Gameiro Da Silva, Towards sustainable, energy-efficient and healthy ventilation strategies in buildings: a review, Renew. Sustain. Energy Rev. (2016), doi:10.1016/j.rser.2016.01.074.
[6] S. Wang, X. Xu, Parameter estimation of internal thermal mass of building dynamic models using genetic algorithm, Energy Convers. Manag. (2006), doi:10.1016/j.enconman.2005.09.011.
[7] J. Karlsson, L. Wadsö, M. Öberg, A conceptual model that simulates the influence of thermal inertia in building structures, Energy Build. (2013), doi:10.1016/j.enbuild.2013.01.017.
[8] D.M. Ogoli, Predicting indoor temperatures in closed buildings with high thermal mass, Energy Build. (2003), doi:10.1016/S0378-7788(02)00246-3.

[9] B.V. Andjelković, B.V. Stojanović, M.M. Stojiljković, J.N. Janevski, M.B. Stojanović, Thermal mass impact on energy performance of a low, medium, and heavy mass building in Belgrade, Therm. Sci. (2013), doi:10.2298/TSCI120409182A.

[10] M. Bojić, M. Miletić, L. Bojić, Optimization of thermal insulation to achieve energy savings in low energy house (refurbishment), Energy Convers. Manag. (2014), doi:10.1016/j.enconman.2014.04.095.

[11] T. Li, J. Song, X. Zhao, Z. Yang, G. Pastel, S. Xu, et al., Anisotropic, lightweight, strong, and super thermally insulating nanowood with naturally aligned nanocellulose, Sci. Adv. (2018), doi:10.1126/sciadv.aar3724.

[12] B. Wicklein, A. Kocjan, G. Salazar-Alvarez, F. Carosio, G. Camino, M. Antonietti, et al., Thermally insulating and fire-retardant lightweight anisotropic foams based on nanocellulose and graphene oxide, Nat. Nanotechnol. (2015), doi:10.1038/nnano.2014.248.

[13] G. Salvalai, J. Pfafferott, M.M. Sesana, Assessing energy and thermal comfort of different low-energy cooling concepts for non-residential buildings, Energy Convers. Manag. (2013), doi:10.1016/j.enconman.2013.07.064.

[14] W. Lin, Z. Ma, M.I. Sohel, P. Cooper, Development and evaluation of a ceiling ventilation system enhanced by solar photovoltaic thermal collectors and phase change materials, Energy Convers. Manag. (2014), doi:10.1016/j.enconman.2014.08.019.

[15] R. Khanal, C. Lei, Solar chimney-a passive strategy for natural ventilation, Energy Build. (2011), doi:10.1016/j.enbuild.2011.03.035.

[16] D.J. Harris, N. Helwig, Solar chimney and building ventilation, Appl. Energy (2007), doi:10.1016/j.apenergy.2006.07.001.

[17] X.Q. Zhai, Z.P. Song, R.Z. Wang, A review for the applications of solar chimneys in buildings, Renew. Sustain. Energy Rev. (2011), doi:10.1016/j.rser.2011.07.013.

[18] C. Tonelli, M. Grimaudo, Timber buildings and thermal inertia: open scientific problems for summer behavior in Mediterranean climate, Energy Build. (2014), doi:10.1016/j.enbuild.2013.12.063.

[19] F. Calise, M.D. D'Accadia, L. Vanoli, Thermoeconomic optimization of solar heating and cooling systems, Energy Convers. Manag. (2011), doi:10.1016/j.enconman.2010.10.025.

[20] S.K. Chou, K.J. Chua, J.C. Ho, A study on the effects of double skin façades on the energy management in buildings, Energy Convers. Manag. (2009), doi:10.1016/j.enconman.2009.05.003.

[21] H. Takebayashi, E. Ishii, M. Moriyama, A. Sakaki, S. Nakajima, H. Ueda, Study to examine the potential for solar energy utilization based on the relationship between urban morphology and solar radiation gain on building rooftops and wall surfaces, Sol. Energy (2015), doi:10.1016/j.solener.2015.05.039.

[22] Z. Yang, X.H. Li, Y.F. Hu, Study on solar radiation and energy efficiency of building glass system, Appl. Therm. Eng. (2006), doi:10.1016/j.applthermaleng.2005.06.012.

[23] D. Lazos, A.B. Sproul, M. Kay, Optimisation of energy management in commercial buildings with weather forecasting inputs: a review, Renew. Sustain. Energy Rev. (2014), doi:10.1016/j.rser.2014.07.053.

[24] A. Ibrahim, A. Fudholi, K. Sopian, M.Y. Othman, M.H. Ruslan, Efficiencies and improvement potential of building integrated photovoltaic thermal (BIPVT) system, Energy Convers. Manag. (2014), doi:10.1016/j.enconman.2013.10.033.

[25] S.W. Lee, C.H. Lim, E.@ Salleh, I Bin. Reflective thermal insulation systems in building: a review on radiant barrier and reflective insulation, Renew. Sustain. Energy Rev. (2016), doi:10.1016/j.rser.2016.07.002.

[26] S. Pashiardis, S.A. Kalogirou, A. Pelengaris, Statistical analysis for the characterization of solar energy utilization and inter-comparison of solar radiation at two sites in Cyprus, Appl. Energy (2017), doi:10.1016/j.apenergy.2017.01.018.

[27] E. Cuce, S.B. Riffat, C.H. Young, Thermal insulation, power generation, lighting and energy saving performance of heat insulation solar glass as a curtain wall application in Taiwan: a comparative experimental study, Energy Convers. Manag. (2015), doi:10.1016/j.enconman.2015.02.062.

[28] K. Kazmierczak, Review of curtain walls, focusing on design problems and solutions. A New Des Paradig Energy Effic Build 2010.

[29] C. Bouden, Influence of glass curtain walls on the building thermal energy consumption under Tunisian climatic conditions: the case of administrative buildings, Renew. Energy (2007), doi:10.1016/j.renene.2006.01.007.

[30] M.L. Persson, A. Roos, M. Wall, Influence of window size on the energy balance of low energy houses, Energy Build. (2006), doi:10.1016/j.enbuild.2005.05.006.

[31] S.K. Alghoul, H.G. Rijabo, M.E. Mashena, Energy consumption in buildings: a correlation for the influence of window to wall ratio and window orientation in Tripoli, Libya, J. Build. Eng. (2017), doi:10.1016/j.jobe.2017.04.003.

[32] M. Thalfeldt, E. Pikas, J. Kurnitski, H. Voll, Facade design principles for nearly zero energy buildings in a cold climate, Energy Build. (2013), doi:10.1016/j.enbuild.2013.08.027.

[33] J. Jie, Y. Hua, H. Wei, P. Gang, L. Jianping, J. Bin, Modeling of a novel Trombe wall with PV cells, Build. Environ. (2007), doi:10.1016/j.buildenv.2006.01.005.

[34] B.K. Koyunbaba, Z. Yilmaz, K. Ulgen, An approach for energy modeling of a building integrated photovoltaic (BIPV) Trombe wall system, Energy Build. (2013), doi:10.1016/j.enbuild.2011.06.031.

[35] D. Chemisana, Building integrated concentrating photovoltaics: a review, Renew. Sustain. Energy Rev. (2011), doi:10.1016/j.rser.2010.07.017.

[36] I. Cerón, E. Caamaño-Martín, F.J. Neila, State-of-the-art" of building integrated photovoltaic products, Renew. Energy (2013), doi:10.1016/j.renene.2013.02.013.

[37] T. James, A. Goodrich, M. Woodhouse, R. Margolis, S. Ong, Building-Integrated integrated photovoltaics (BIPV) in the residential sector: aAn analysis of installed rooftop system prices. Tech Rep NREL/TP-6A20-53103 2012.

[38] O. Saadatian, K. Sopian, C.H. Lim, N. Asim, M.Y. Sulaiman, Trombe walls: a review of opportunities and challenges in research and development, Renew. Sustain. Energy Rev. (2012), doi:10.1016/j.rser.2012.06.032.

[39] S. Jaber, S. Ajib, Optimum design of Trombe wall system in mediterranean region, Sol. Energy (2011), doi:10.1016/j.solener.2011.04.025.

[40] G. Gan, A parametric study of Trombe walls for passive cooling of buildings, Energy Build. (1998), doi:10.1016/S0378-7788(97)00024-8.

[41] R. Luthander, J. Widén, D. Nilsson, J. Palm, Photovoltaic self-consumption in buildings: a review, Appl. Energy (2015), doi:10.1016/j.apenergy.2014.12.028.

[42] A. Marucci, D. Monarca, M. Cecchini, A. Colantoni, E. Allegrini, A. Cappuccini, Use of semi-transparent photovoltaic films as shadowing systems in mediterranean greenhouses, Lect. Notes Comput. Sci. (including Subser. Lect. Notes Artif. Intell. Lect. Notes Bioinformatics) (2013), doi:10.1007/978-3-642-39643-4_18.

[43] L.A. Burlacu, Natural light and building materials, Mater. Res. Appl. PTS (2014) 1–3 10.4028/www.scientific.net/AMR.875-877.1954.

[44] A.P. Raman, M.A. Anoma, L. Zhu, E. Rephaeli, S. Fan, Passive radiative cooling below ambient air temperature under direct sunlight, Nature (2014), doi:10.1038/nature13883.

[45] L. Zhu, A. Raman, K.X. Wang, M.A. Anoma, S. Fan, Radiative cooling of solar cells, Optica (2014), doi:10.1364/OPTICA.1.000032.

[46] E.A. Goldstein, A.P. Raman, S. Fan, Sub-ambient non-evaporative fluid cooling with the sky, Nat. Energy (2017), doi:10.1038/nenergy.2017.143.

[47] P.C. Hsu, A.Y. Song, P.B. Catrysse, C. Liu, Y. Peng, J. Xie, et al., Radiative human body cooling by nanoporous polyethylene textile, Science (80–) (2016), doi:10.1126/science.aaf5471.

[48] M.M. Hossain, M. Gu, Radiative cooling: principles, progress, and potentials, Adv. Sci. (2016), doi:10.1002/advs.201500360.

[49] J. Mandal, Y. Fu, A.C. Overvig, M. Jia, K. Sun, N.N. Shi, et al., Hierarchically porous polymer coatings for highly efficient passive daytime radiative cooling, Science (80–)) (2018), doi:10.1126/science.aat9513.

[50] K.L. Uemoto, N.M.N. Sato, V.M. John, Estimating thermal performance of cool colored paints, Energy Build. (2010), doi:10.1016/j.enbuild.2009.07.026.

[51] H.F. Castleton, V. Stovin, S.B.M. Beck, J.B. Davison, Green roofs; building energy savings and the potential for retrofit, Energy Build. (2010), doi:10.1016/j.enbuild.2010.05.004.

[52] J. Zhu, B. Chen, Simplified analysis methods for thermal responsive performance of passive solar house in cold area of China, Energy Build. (2013), doi:10.1016/j.enbuild.2013.07.038.

[53] J. Zhu, B. Chen, Experimental study on thermal response of passive solar house with color changed, Renew. Energy (2015), doi:10.1016/j.renene.2014.05.062.

[54] M. Hajzeri, K. Bašnec, M. Bele, M.K. Gunde, Influence of developer on structural, optical and thermal properties of a benzofluoran-based thermochromic composite, Dye Pigment (2015), doi:10.1016/j.dyepig.2014.10.014.

[55] T. Karlessi, M. Santamouris, Improving the performance of thermochromic coatings with the use of UV and optical filters tested under accelerated aging conditions, Int. J. Low-Carbon Technol. (2015), doi:10.1093/ijlct/ctt027.

[56] C. Wang, Y. Zhu, J. Qu, H.D. Hu, Automatic air temperature control in a container with an optic-variable wall, Appl. Energy (2018) 224, doi:10.1016/j.apenergy.2018.05.018.

[57] C. Wang, X. Guo, Y. Zhu, Energy saving with optic-variable wall for stable air temperature control, Energy 173 (2019) 38–47, doi:10.1016/j.energy.2019.02.051.

[58] C. Wang, Y. Zhu, X. Guo, Thermally responsive coating on building heating and cooling energy efficiency and indoor comfort improvement, Appl Energy 253 (2019) 113506, doi:10.1016/J.APENERGY.2019.113506.

[59] R.J. de Dear, G.S. Brager, Thermal comfort in naturally ventilated buildings: revisions to ASHRAE Standard 55, Energy Build. 34 (2002) 549–561, doi:10.1016/S0378-7788(02)00005-1.